Analyst

PAPER

View Article Online
View Journal

Cite this: DOI: 10.1039/c7an01506b

Ambient-air ozonolysis of triglycerides in aged fingerprint residues†

Stefanie Pleik,[a,b] Bernhard Spengler,[b] Dhaka Ram Bhandari,[b] Steven Luhn,[a] Thomas Schäfer,[a] Dieter Urbach[a] and Dieter Kirsch*[a]

In forensic science, reconstructing the timing of events occurring during a criminal offense is of great importance. In some cases, the time when particular evidence was left on a crime scene is a critical matter. The ability to estimate the fingerprint age would raise the evidentiary value of fingerprints tremendously. For this purpose the most promising approach is the analysis of changes in the chemical compositions of fingerprint residues in the course of aging. The focus of our study is the identification of human specific compounds in fingerprint residues, characterized by a significant aging behavior that could analytically be used for the age determination of fingerprints in future. The first challenge is the sensitive detection of trace amounts of relevant human specific fingerprint compounds. Highly sensitive LC-MS methods were developed for the reliable structure identification of unsaturated triglycerides and their natural degradation products in order to proof the aging mechanism that takes place in fingerprint residues. Thus our results build the fundamental basis for further forensic method development and potential application in forensic investigation. Ozonolysis was found to be one of the major lipid degradation pathways in fingerprint residues in ambient air. High-resolution tandem mass spectrometry ($HRMS^2$) was carried out to identify the ozonolysis products (TG48:0-monoozonide) formed under exposure to the highly reactive ozone in atmospheric air. The obtained products were confirmed by matrix assisted laser desorption ionization mass spectrometry imaging (MALDI-MSI). Despite several challenges and limitations in the age estimation of fingerprints, the identification of individual degradation products of specific unsaturated lipids in aged fingerprint samples represents a significant analytical progress, resulting in a strong increase in the validity of chemical analysis of fingerprints.

Received 11th September 2017,
Accepted 12th January 2018

DOI: 10.1039/c7an01506b

rsc.li/analyst

Introduction

Fingerprint residues are a complex mixture of compounds originating from various sources. This study focuses on lipids in fingerprint residues, produced by sebaceous glands. The chemical composition of human sebum is dominated by free fatty acids, triglycerides and wax ester.[1–9]

Analytical investigations of fingerprint residues are usually performed using gas chromatography mass spectrometry (GC-MS). In addition to GC-MS, mass spectrometric, spectroscopic or optical methods are used in fingerprint chemistry.[10–24] The literature on fingerprint residues focused on the detection and analysis of chemical composition,[10,12] donor classification according to their compositional profiles,[15–18] gender determination[14] and age estimation.[19–22,25,26]

Initial attempts to develop analytical methods to estimate the age of fingerprint residues were based on the degradation of compounds in residues with time.[10,19,21,22,25] GC-MS was used to analyze the degradation rates of squalene, cholesterol, lipids and other unsaturated compounds present in fingerprint residues. However, due to the high variability of fingerprint compositions, analyzing and quantifying the absolute amount of initial compounds is not a reliable method to estimate the age of the fingerprint. Signal intensity ratios were proposed as being independent of the absolute amount of residues and therefore might be beneficial to define markers for fingerprint aging.[21,22,25]

While studying the aging behavior of the selected target compounds in fingerprints, Girod *et al.* found various influencing factors including environmental conditions that strongly affect the aging of individual compounds.[25] In practice, Girod *et al.* differentiated between known influencing factors and unknown factors in real cases. These factors are known to affect the aging behavior of particular compounds tremendously.[25]

[a]*Forensic Science Institute, Federal Criminal Police Office, 65173 Wiesbaden, Germany. E-mail: dieter.kirsch@bka.bund.de*
[b]*Institute of Inorganic and Analytical Chemistry, Justus Liebig University Giessen, Heinrich-Buff-Ring 17, 35392 Giessen, Germany*

†Electronic supplementary information (ESI) available. See DOI: 10.1039/c7an01506b

Without prior knowledge of aging conditions, an age estimation of fingerprint samples in practice seems to be impossible. So, it is crucial to build aging models for each degradation pathway under changing conditions to pin out the relevant factors. The challenges associated with the age determination of fingerprint residues are well described by Girod *et al.*[26,27]

In our previous study, we reported the identification of fatty acid degradation products in aged fingerprint residues.[28] Decanal was found in aged fingerprint samples as a major aging product of unsaturated fatty acids. In addition, oxoacids were identified as fatty acid degradation products, indicating the chain length and the double bond position of initially unreacted unsaturated fatty acids. Additionally, we identified two unsaturated fatty acids with high signal intensity in fingerprint residues as the human specific Δ6-hexadecenoic acid and Δ8-octadecenoic acid. With these findings, we are able to generate relative values as aging markers, which are independent of the absolute amount of fingerprint residues. Signal intensity ratios provide the most reliable information about the age of a fingerprint. The essential advantage of our findings is the relative signal intensity value which is based on the degradation of one single and unique fingerprint ingredient. The general lack of aging models that include the effects of certain influences on the aging of individual compounds so far limits the use of reported results in forensic case work.

Here, we investigate the degradation of lipids in fingerprint residues in atmospheric air. In 1965 Frankel already described the mechanisms of different types of lipid oxidations[29] and in the following years several additional mechanistic studies on the autoxidation of polyunsaturated fatty acids and related lipids were published.[30–35] Lipid oxidation is divided into enzymatic and non-enzymatic degradation, and both may be useful for determining the fingerprint age. In both, enzymatic and non-enzymatic degradation, secondary products are aldehydes that are highly reactive to amino acids and could provide a distinctive biochemical age marker.[36–41] Additionally, given that fingerprint residues age under ambient conditions, the oxidation due to ozone should be considered.

The possible degradation pathways for fingerprint residue lipids are numerous. Many aging reactions occur simultaneously, which leads to low concentrations of some degradation products. Since ozone is a highly reactive pollutant gas in ambient (including indoor) air we focused on understanding the degradation pathways of lipid ozonolysis.

Based on early achievements[42–45] current ozonolysis studies are being conducted for a variety of different purposes. Combined with electrospray ionization tandem mass spectrometry (ESI-MS^2), ozone induced dissociation (OzID) of unsaturated compounds/lipids is a powerful method for structure identification and determination of lipid double bond positions.[46]

Multiple studies analyze lipid samples oxidized by artificial ozone.[46–55] Weschler *et al.* studied the volatile products from squalene ozonolysis out of human skin lipid samples.[56] The ozonolysis of squalene is also a part of the studies of Baldi *et al.*,[57] in which they discovered a large number of squalene oxidation products.

Although ozone is an air pollutant (concentration range between 20 and 60 parts per billion) even in indoor environments,[58,59] there are a few studies about lipid ozonolysis under ambient conditions. Blanksby *et al.* observed lipids reacting with the low concentrations of ozone in ambient air by analyzing lipids and ozonolysis products directly from surfaces by desorption electrospray ionization-mass spectrometry (DESI-MS) coupled to thin layer chromatography (TLC).[60]

Lipid oxidation is well discussed in the literature. However, the quantification of the specific compounds produced from aging fingerprints is difficult, due to the high diversity and limited stability of the already small amounts of the compounds produced. Consequently, analytical methodologies require high sensitivity, specificity and accuracy. There are a multitude of conceivable analytical techniques that could provide the sensitive and reliable identification of lipid degradation compounds. These techniques include different spectrometric and spectroscopic methods as well as numerous separation protocols and derivatization techniques.[53,61–71]

Besides GC- and LC-MS methods for the detection and identification of fingerprint residue compounds, imaging experiments of fingerprints are also an area of interest in forensic science. Spectroscopic and spectrometric methods were used for the determination of spatial distributions of compounds in fingerprints. Merkel *et al.* developed a method using chromatic white light sensors to obtain high resolution images of aged and non-aged fingerprint samples.[72] Cooks *et al.* were among the first to employ MS-imaging in forensic analysis.[73] In 2009 Francese and colleagues analyzed endogenous lipids in fingerprints for the first time by MALDI MS imaging (MSI) and monitored the degradation of oleic acid with aging.[74] The potential of MALDI-imaging for fingerprint analysis in forensic science was recently reviewed. MALDI-imaging was described to be suitable for the detection of endogenous compounds as well as exogenous compounds, such as drugs and illicit substances. Also provided was a MSI protocol that should be compatible with the forensic casework.[75] Francese *et al.* also used MALDI-MSI to analyze the peptides produced by the tryptic digestion of fingerprints.[76] In a study by Elsner *et al.* gold nanoparticles were applied to fingerprints prior to MS-analysis.[77] Comprehensive chemical composition analyses of fingerprints were performed using laser desorption ionization, MALDI and sputtering methods by Lauzon *et al.*[78] Yagnik *et al.* combined accurate mass detection by obtaining fragment spectra through high resolution mass spectrometry and subsequent compound identification by low resolution tandem mass spectrometry, in a multiplex method of fingerprint analysis and imaging.[79] The diffusion of sebum molecules in fingerprints in the course of aging was analyzed by TOF-SIMS imaging as a potential aging marker.[80] Other groups focused on the detection of exogenous materials in fingerprints, such as illicit drugs or pharmaceuticals by MS-imaging.[81,82]

In this study, MALDI MS imaging was conducted on aged fingerprints to prove that triglyceride ozonolysis products exist in the fingerprint pattern, to confirm the authenticity of the

obtained LC-MS results and to show the high potential of this technique for future forensic investigations.

Materials and methods

Chemicals and materials

LiChrosolv® grade solvents (methanol, 2-propanol, acetonitrile, water, dichloromethane, chloroform) for sample extraction, sample preparation and LC measurements were purchased from Merck KGaA (Darmstadt, Germany). Ammonium formate (Fluka, ≥99.0% for HPLC) was purchased from Sigma Aldrich Chemie GmbH (Taufkirchen, Germany). It was used as 1 mol L^{-1} aqueous solution for post-column ionization to obtain ammonium adducts of ionized lipids. Trioctadecenoyl glycerol (≥99%) was purchased as a standard lipid from Sigma Aldrich Chemie GmbH (Taufkirchen, Germany). Aluminum foil (thickness 15 μm) as a substrate for aging experiments was purchased from Carl Roth GmbH & Co. KG (Karlsruhe, Germany).

HPLC grade acetone, water and 2,5-dihydroxybenzoic acid (2,5-DHB) for MALDI sample preparation were purchased from Merck KGaA (Darmstadt, Germany). Trifluoroacetic acid (TFA) was purchased from AppliChem GmbH (Darmstadt, Germany).

Sample preparation for LC measurements

Trioctadecenoyl glycerol stock solution was prepared in dichloromethane at a concentration of 1 mmol L^{-1}. Pieces of aluminum foil (2 × 2 cm) were each coated with 3 μL of the stock solution for aging experiments. During aging, the samples were exposed to light (daytime) and to darkness (night) to mimic typical light exposure. The room temperature was held constant at 20 °C (±1 °C). The samples were analyzed after 0 hours, two hours and two days of aging. After the desired sample age was reached, foils were folded and placed in separate glass vials for extraction. The compounds were extracted with 200 μL chloroform and were mixed on a vortex mixer. After extraction, aluminum foil was removed from the glass vial and discarded. Chloroform was evaporated under nitrogen flux to dryness and the remaining residue was dissolved in 50 μL 2-propanol for LC analysis.

For fingerprint sample preparation, three donors (two females, one male) placed their fingertips on pieces (2 × 2 cm) of aluminum foil (20 fingerprints from each donor), preceded by the so-called fingerprint grooming.[19] One piece of aluminum foil was used for one single fingerprint. For the grooming procedure, donors wiped their fingertips over their forehead, nose, chin, and scalp. 30 samples (10 fingerprints from each donor) and 10 trioctadecenoyl glycerol samples (prepared as reported above) were stored in open Petri dishes on the lab bench during the aging process. The samples were exposed to light during daytime and to darkness during night to mimic typical light exposure. An additional 30 samples (10 fingerprints from each donor) and 10 trioctadecenoyl glycerol samples were stored in open Petri dishes in the drawer of a cupboard. These samples were protected from light. The room temperature was 20 °C (±1 °C). Every sample was deep frozen after the desired sample age was reached. Fingerprint samples and trioctadecenoyl glycerol samples from both storage conditions were analyzed after 0, 1, 3, 6, 8, 10, 14, 16, 24 and 63 days of aging. For analysis foil samples were folded and placed in separate glass vials for extraction. The compounds were extracted with 200 μL chloroform and were mixed on a vortex mixer. After extraction, aluminum foil was removed from the vial and discarded. A chloroform-based sample was mixed with 200 μL water for liquid–liquid extraction to clean up the samples. Afterwards the aqueous phase was discarded and the organic phase was evaporated to dryness under nitrogen flux. The remaining residue was dissolved in 50 μL 2-propanol for LC analysis. In total 60 fingerprint samples and 20 trioctadecenoyl glycerol samples were analyzed by the reported method. For instrument qualification a control substance was measured regularly after every 10 samples.

Sample preparation for MALDI measurements

Fingerprints from one female donor were deposited on glass slides, preceded by the described fingerprint grooming.[19] Optical images of the non-aged fingerprints were generated prior to matrix application by using a digital microscope (Keyence VHX-5000 digital, Keyence Deutschland GmbH, Neu-Isenburg, Germany) equipped with digital objectives (VH-Z250T, VHX-J250T), a motorized sample stage and a digital camera (VHX-5020 CMOS). For aging, the samples were stored in open Petri dishes on the lab bench. The samples were exposed to light during daytime and to darkness during night to mimic typical light exposure. The fingerprint sample aged for 26 days was chosen for analysis because of the ideal signal intensity of relevant compounds. After an appropriate sample age (26 days) was reached, optical images of the aged fingerprints were generated prior to matrix application by using the above-mentioned digital microscope.

The matrix was prepared at a concentration of 30 mg mL^{-1} of 2,5-DHB in acetone/water 1 : 1 v/v (0.1% TFA). Then 2,5-DHB solution was sprayed onto the fingerprint sample by using an automated device (SMALDIPrep, TransMIT GmbH, Giessen, Germany).[83] It provided the uniform application of a 100 μL matrix on the sample with a spray rate of 10 μL min^{-1}. Nitrogen gas was adjusted to 1 bar.

Instrumentation and methods

LC separations were carried out on an UltiMate® 3000 UHPLC (Dionex Softron GmbH, Thermo Fisher Scientific GmbH, Germering, Germany) equipped with a NUCLEODUR® C18 Pyramid reversed-phase column (*L*: 150 mm, ID: 1 mm, particle size: 2.1 μm, Macherey-Nagel GmbH & Co. KG, Düren, Germany). For lipid separation, several solvents, binary solvents (water, acetonitrile, methanol, 1-butanol, 2-propanol) and different gradients were tested for the analyses of fingerprint residues. Best separation results were achieved with methanol as mobile phase A and 2-propanol as mobile phase B. The gradient is described in ESI Table S1.†

Compound separation by using the reported gradient results in sharp peaks without carry over effects.

Post-column ionization with ammonium formate (1 mol L^{-1}) was carried out by using a syringe pump (KDS100, KD Scientific Inc., Holliston, MA, USA) which provides continuous flow in the ESI source with a flow rate of 50 μL h^{-1}.

For the LC-MS analyses the UHPLC was attached to the hybrid mass spectrometer QToF-compact (Bruker Daltonik GmbH, Bremen, Germany, max. resolution 24 000) equipped with an ESI source. ESI source parameters are presented in ESI Table S2.†

Spectra were recorded with a rate of 1 Hz in positive ion mode in the mass range of *m*/*z* 80–1200. Adjusted tune parameters are presented in ESI Table S3.† Negative ion mode was tested on other instruments, but the signal intensity of the detected compounds was too low for reliable structure identification.

For MALDI imaging experiments a high resolution imaging ion source, (AP-SMALDI10, TransMIT GmbH, Giessen, Germany),[84] operating at atmospheric pressure and coupled to a high resolution mass spectrometer (Q-Exactive, Thermo Fisher Scientific, GmbH, Bremen, Germany) was used.

A nitrogen laser operating at a repetition rate of 60 Hz was used for the desorption and ionization of the analytes. The imaging experiments were performed at a step size of 25 μm. The ions formed by 30 laser pulses were accumulated in the C-trap prior to transferring them to the Orbitrap mass analyzer. The mass resolution was set at 140 000@*m*/*z* 200. Mass spectra were generated in the mass range of *m*/*z* 250 to 1000 in the positive ion mode. The matrix cluster ion at *m*/*z* 716.12461 was used as a lock mass. The negative ion mode was tested by using another matrix, but the signal intensity of detected compounds was too low for reliable identification.

Data processing

LC-MS results were evaluated by the software Bruker Compass DataAnalysis 4.2 (Bruker Daltonik GmbH, Bremen, Germany). An in-house developed software package (MIRION)[85] was used to generate MS images and to calculate accurate masses. For image generation, a narrow mass bin width (±5 ppm) was used. The images were not normalized or interpolated. Mass accuracy of better than 3 ppm was used for compound assignment.

Ethical statement

The Forensic Science Institute of the Federal Criminal Police Office (Bundeskriminalamt) confirms that all experiments/studies were performed in compliance with the guidelines of the Bundeskriminalamt. The Forensic Science Institute of the Bundeskriminalamt approved these experiments/studies. The authors received informed consent for use of the fingerprints from fingerprint donors.

Results and discussion

LC-MS: standard lipid trioctadecenoyl glycerol

Aging experiments were carried out with the standard lipid trioctadecenoyl glycerol TG(54:3), in order to identify the major degradation pathway and the corresponding reaction mechanism of unsaturated triglycerides in atmospheric air. The lipid bears three unsaturated fatty acid chains and thus provides three different oxidation sites. Fig. 1 shows the structure of trioctadecenoyl glycerol **1** and conceivable oxidation products **2–4** in consideration of the Criegee mechanism for lipid ozonolysis.[44,45]

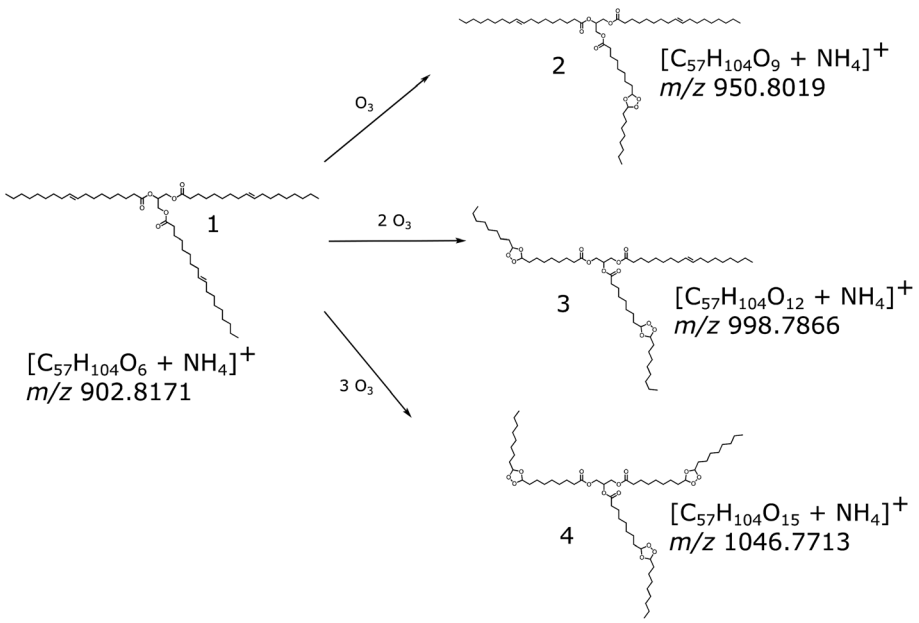

Fig. 1 Triglyceride ozonolysis. Three different ozonolysis products (**2–4**) of trioctadecenoyl glycerol (**1**) in consideration of the Criegee mechanism. Exact masses for NH_4^+-adduct ions are provided.

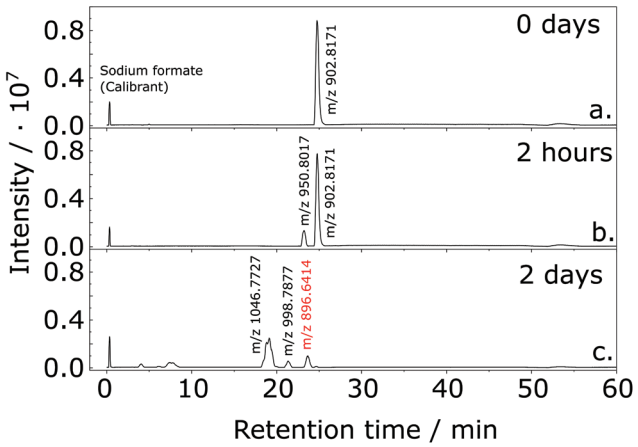

Fig. 2 Total ion count (TIC) diagrams of non-aged and aged samples of trioctadecenoyl glycerol from the reference material. (a) Non-aged sample. (b) 2 hour aged sample (c) 2 day aged sample.

The LC-MS results of non-aged and aged trioctadecenoyl glycerol samples show a time dependent oxidation of trioctadecenoyl glycerol (Fig. 2). After only two hours of sample aging, the monooxidation of TG(54:3) could be observed. Besides the unreacted lipid (*m*/*z* 902.8171, $[C_{57}H_{104}O_6 + NH_4]^+$, RT: 24.8 min), the lipid monoozonide ($[C_{57}H_{104}O_9 + NH_4]^+$, *m*/*z* 950.8017, RT: 23.2 min) was detected. After 2 days of aging the lipid diozonide ($[C_{57}H_{104}O_{12} + NH_4]^+$, *m*/*z* 998.7877, RT: 21.3 min) and the lipid triozonide ($[C_{57}H_{104}O_{15} + NH_4]^+$, *m*/*z* 1046.7727, RT: 19.1 min) were additionally detected. When the sample age reached 2 days, the unreacted lipid fell below the limit of detection. With proceeding degradation, the lipid triozonide became the major oxidation product, indicating the complete degradation of the original unsaturated lipid.

In the sample, aged two days, a doubly charged ion (*m*/*z* 896.6414, *z* = 2, RT: 23.3 min) was detected in addition to ozonolysis products. The reaction between the intermediates of lipid ozonides is known to produce high molecular weight compounds with molecular weights up to 2000 Da.[50] The detection of these additional degradation products indicates concurrent reaction pathways during the aging of triglycerides. The structure of the ion at *m*/*z* 896.6414 could not be entirely determined. This type of aging process should be the subject of further investigations in fingerprint chemistry.

Tandem mass spectrometry was used for structure identification of the detected lipid ozonides. Fig. 3 shows the MS^2 spectrum and the structures of relevant fragment ions of the observed monoozonide at *m*/*z* 950.8019. The elimination of the oxidized fatty acid chain in course of fragmentation results in the signal at *m*/*z* 603.5338 (marked blue). The ion signal at *m*/*z* 339.2897 (marked green) was identified as octadecenoic acid attached to the glyceryl backbone, verifying the fatty acid chain lengths. The signal at *m*/*z* 493.3892 (marked red) was identified as bearing octadecenoic acid attached to the oxidized fatty acid chain which was cleaved at the oxidized carbon. As the cleaved oxidized chain at *m*/*z* 493.3892 still contains nine carbon atoms, it is the first proof of the double bond position on C9. The same cleavage with the other fragment containing the charge was detected as an ion signal at *m*/*z* 176.1644 (marked grey), which also contains nine carbon atoms. It additionally proves the C9 double bond position in the original lipid. These characteristic fragments allow the identification of structural details including the fatty acid chain length, double bond position and oxidation site. It

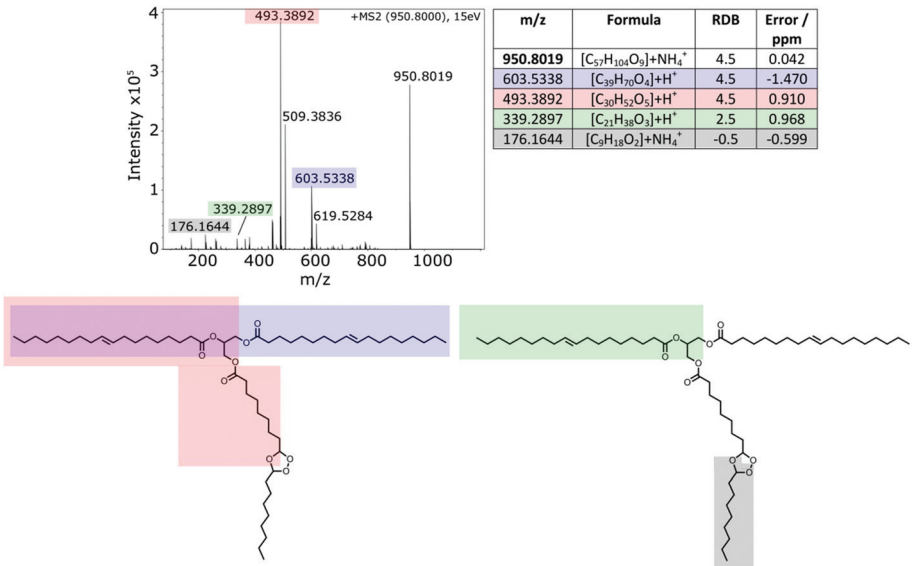

m/z	Formula	RDB	Error / ppm
950.8019	$[C_{57}H_{104}O_9]+NH_4^+$	4.5	0.042
603.5338	$[C_{39}H_{70}O_4]+H^+$	4.5	-1.470
493.3892	$[C_{30}H_{52}O_5]+H^+$	4.5	0.910
339.2897	$[C_{21}H_{38}O_3]+H^+$	2.5	0.968
176.1644	$[C_9H_{18}O_2]+NH_4^+$	-0.5	-0.599

Fig. 3 MS^2 spectrum of *m*/*z* 950.8019. In addition to exact masses, formulae, ring double bond (RDB) equivalents and mass accuracy are provided in the table. Structures of relevant fragments are colored and highlighted in the structure of TG(54:2)-monoozonide. Mass accuracy is given as Δm in ppm $\left(\Delta m = \frac{m_{calculated} - m_{measured}}{m_{calculated}}\right)$.

builds the basis for the identification of similar degradation products in fingerprint samples. Exact structures of proposed fragments are provided in ESI Table S4.†

LC-MS: fingerprint samples

The fingerprint samples were analyzed by LC-MS (Fig. 4) to study the lipid oxidation in fingerprint samples and to elucidate the structure of products. Due to the high diversity of compounds in fingerprint residues, a huge number of lipid signals were obtained between 20 and 30 minute retention time. Using the accurate mass detection, several signals in the non-aged fingerprint samples were identified as the homologous series of saturated and unsaturated triglycerides. Our studies focused on the triglyceride trihexadecanoyl glycerol (named TG(48:0)) and its unsaturated derivatives (TG(48:1), TG (48:2), TG(48:3)), shown as extracted ion chromatograms in Fig. 4(a–d). The monounsaturated dihexadecanoyl-hexadecenoyl glycerol (Fig. 4b) exhibited high signal intensities in fresh fingerprint samples and thus the present studies focused on its aging behavior and the structure identification of its oxidation product. The compound is called TG(48:1) in the following.

Based on the findings from aging experiments with the standard lipid trioctadecenoyl glycerol (TG(54:3)) we were able to calculate the theoretical mass for the expected oxidation product of fingerprint lipid TG(48:1). In lipid ozonolysis, the formula of the desired oxidation product can be assumed as $C_{51}H_{96}O_9$ (named TG(48:0)-monoozonide) with calculated *m/z* 870.7393 (as NH_4^+ adduct). Fig. 5 shows the extracted ion chromatograms from LC-MS experiments for the ammonium adducts with the masses of TG(48:0) (*m/z* 824.7719, Δm = 2.102 ppm), TG(48:1) (*m/z* 822.7550, Δm = 0.588 ppm) and TG(48:0)-monoozonide (*m/z* 870.7395, Δm = 0.276 ppm) in three different aged fingerprint samples. Fig. 5a shows the unreacted sample, Fig. 5b shows a fingerprint sample after 10 days of aging and Fig. 5c shows a fingerprint sample aged 63 days. Signal intensities of TG(48:0) and TG(48:1) shown in Fig. 5a illustrate the highest intensity for the monounsaturated lipid TG(48:1). After 10 days of aging, the ratio of both signal

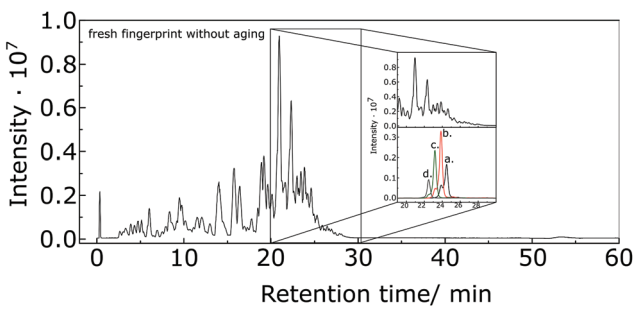

Fig. 4 HPLC separation of lipids in non-aged fingerprint residue. The detailed section between 20 and 30 minute retention time shows the extracted ion chromatograms for (a) *m/z* 824.7719 (Δm = 2.102 ppm), (b) *m/z* 822.7550 (Δm = 0.588 ppm), (c) *m/z* 820.7395 (Δm = 0.772 ppm) and (d) *m/z* 818.7235 (Δm = 0.347 ppm).

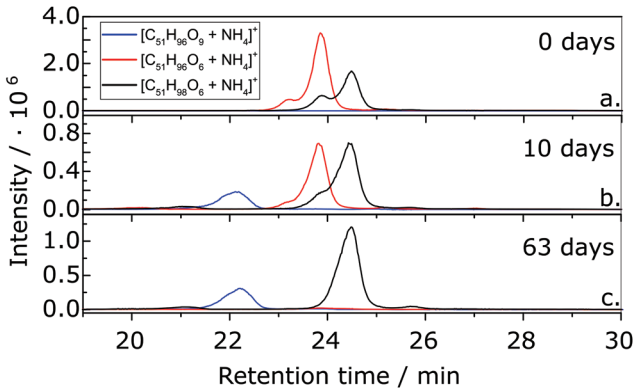

Fig. 5 Extracted ion chromatograms of *m/z* 824.7719 (black), *m/z* 822.7550 (red) and *m/z* 870.7395 (blue) in three fingerprint samples of different ages ((a) 0 days, (b) 10 days and (c) 63 days).

intensities changed, with TG(48:0) and TG(48:1) now exhibiting similar signal intensities in the course of degradation of TG(48:1). In the same analysis of the 10 day old aged sample, the expected degradation product TG(48:0)-monoozonide was detected. With the aging process proceeding up to 63 days, the monounsaturated lipid TG(48:1) was below the limit of detection. The saturated lipid TG(48:0) and the oxidation product TG(48:0)-monoozonide were still detectable in samples after 63 days. Compared to the results from aging experiments with the standard lipid TG(54:3), the fingerprint lipid TG(48:1) was detectable in aged fingerprint samples for much longer after deposition (>10 d) than the standard lipid from the reference material (<2 d). Since the standard lipid TG(54:3) bears three double bonds, compared to the only one in TG(48:1), it can be assumed to be more reactive *versus* oxygen species than the fingerprint lipid. Furthermore, fingerprint residues comprise numerous compounds, some of them with protective properties. These compounds might influence the aging behavior of TG(48:1), giving another explanation for the differences between the aging of the standard lipid and the aging of the fingerprint lipid.

Tandem mass spectrometry was conducted to identify the molecular structures of the oxidation products. The product ion spectrum (Fig. 6) of the precursor ion at *m/z* 870.7395 (TG(48:0)-monoozonoid) exhibits a pattern similar to one of the monooxidized trioctadecenoyl glycerols at *m/z* 950.8017.

Elimination of the complete oxidized fatty acid chain resulted in the fragment ion at *m/z* 551.5028 (marked blue), whereas cleavage at the oxidized carbon atom produced the fragment ion at *m/z* 698.5924 (marked yellow) respectively. The detection of *m/z* 313.2729 (marked green) allows the assignment of hexadecanoic acid in both unreacted fatty acid chains in the triglyceride. Cleavage at the oxidation site in addition to the elimination of one fatty acid chain resulted in the fragment ion at *m/z* 425.3266 (marked red). The fragment ion at *m/z* 190.1791 (marked grey) proves the double bond position in the original lipid at C6. As we were able to identify *m/z* 190.1791, it is verified that the unsaturated fatty acid in the unreacted lipid

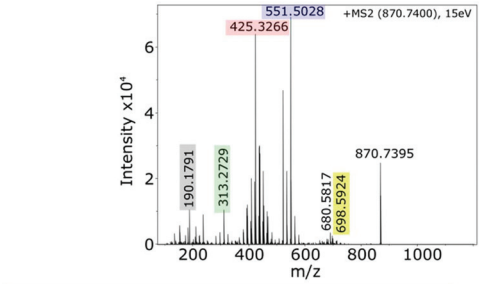

m/z	Formula	RDB	Error / ppm
870.7395	$[C_{51}H_{96}O_9]+NH_4^+$	2.5	0.276
698.5924	$[C_{41}H_{76}O_7]+NH_4^+$	2.5	-0.759
551.5028	$[C_{35}H_{66}O_4]+H^+$	2.5	-1.064
425.3266	$[C_{25}H_{44}O_5]+H^+$	3.5	1.056
313.2729	$[C_{19}H_{36}O_3]+H^+$	1.5	-2.622
190.1791	$[C_{10}H_{20}O_2]+NH_4^+$	-0.5	-5.550

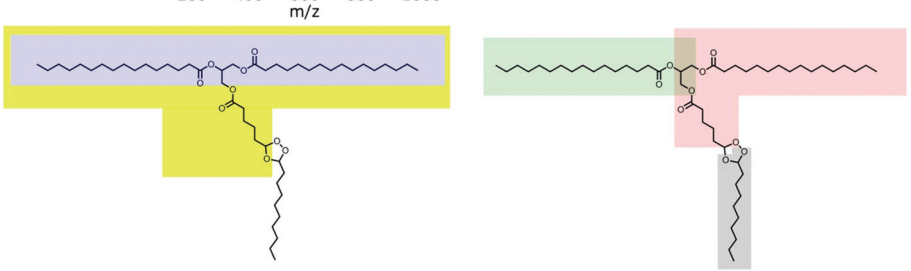

Fig. 6 MS^2 spectrum of *m/z* 870.7395. In addition to exact masses, formula, ring double bond (RDB) equivalents and mass deviation (ppm) are provided in the table. Structures of relevant fragments are colored and highlighted in the structure of TG(48:0)-monoozonide.

was sapienic acid, the fatty acid characteristically found in human sebum. This finding is a valuable improvement for fingerprint chemistry and method development in age determination, as the triglyceride containing sapienic acid is specific to human sebum. Exact structures of proposed fragments are additionally provided in ESI Table S5.†

Since we observed a significant degradation of TG(48:1) within 10 days after the deposition of fingerprints, signal intensities of target compounds were monitored as a function of time. As we detected constant signal intensities for the saturated lipid TG(48:0) during aging (Fig. 5), this compound was used as a natural internal standard for semi-quantitative analysis in following aging experiments presenting the time dependent aging.

In order to estimate the effect of indoor light on the aging behavior of the selected compounds, 30 samples were stored on the lab bench and an additional 30 samples were stored in the drawer, protected from light as much as feasible. Fig. 7 presents the evaluation of the obtained data. In Fig. 7a and b the aging curves of TG(48:1) for three different fingerprint donors (black, red and green) are presented as a function of time. Fig. 7a presents the aging curves for fingerprint samples stored on the lab bench and Fig. 7b presents the aging curves for fingerprint samples stored in the drawer. In some fingerprint samples the target compound TG(48:1) was below the limit of detection, due to the poor quality of the samples. These samples were not included in the generation of aging curves. For the generation of a reliable aging marker, the signal intensity ratios between TG(48:1) and TG(48:0) (as natural internal standards) were determined for the aging curves shown in Fig. 7a and b. Fig. 7a shows the degradation of TG(48:1) after the deposition of fingerprints in every aging curve. This diagram illustrates the tremendous complexity of fingerprint samples produced by different donors. We observed a general trend of signal intensity decrease for TG(48:1) in the course of aging, but the three aging curves differed from each other. The aging curve for donor 1 already ends at 6 days, because TG(48:1) was below the limit of detection in samples older than 6 days. The samples of donor 3 exhibited detectable signal intensities up to 3 days, whereas donor 2 produced very rich samples, and due to very good sample quality, TG(48:1) could still be detected after 24 days of aging. Differences between donor curves can be explained by several influencing factors. Fast degradation may indicate multiple competing degradation pathways for the same unsaturated lipid. On the other hand, slow degradation might be effected by protective substances (*e.g.* from skin care products). Very small amounts of additional unsaturated triglycerides with potential protective properties were detected in fingerprint samples. Due to very low signal intensities, the structure of these compounds cannot be identified reliably by the reported method.

Fig. 7b shows the aging curves of TG(48:1) for the light-protected fingerprint samples. Again, every aging curve showed a general trend of signal intensity decrease, but the degradation of TG(48:1) occurred much slower than in the samples exposed to light.

Fig. 7c shows the formation curves for the degradation product TG(48:0)-monoozonide in the samples stored on the lab bench. Signal intensity ratios between TG(48:0)-monoozonide and TG(48:0) were determined in order to obtain reliable aging values. For all three donors, a fast signal intensity increase was measured within 3 days of aging. With proceeding age the signal intensities of TG(48:0)-monoozonide stayed constant. These results are in conformance with aging curves shown in Fig. 7a. Within the first 3 days of aging, signal intensities of TG(48:1) strongly decreased while signal intensities of the corresponding degradation product increased.

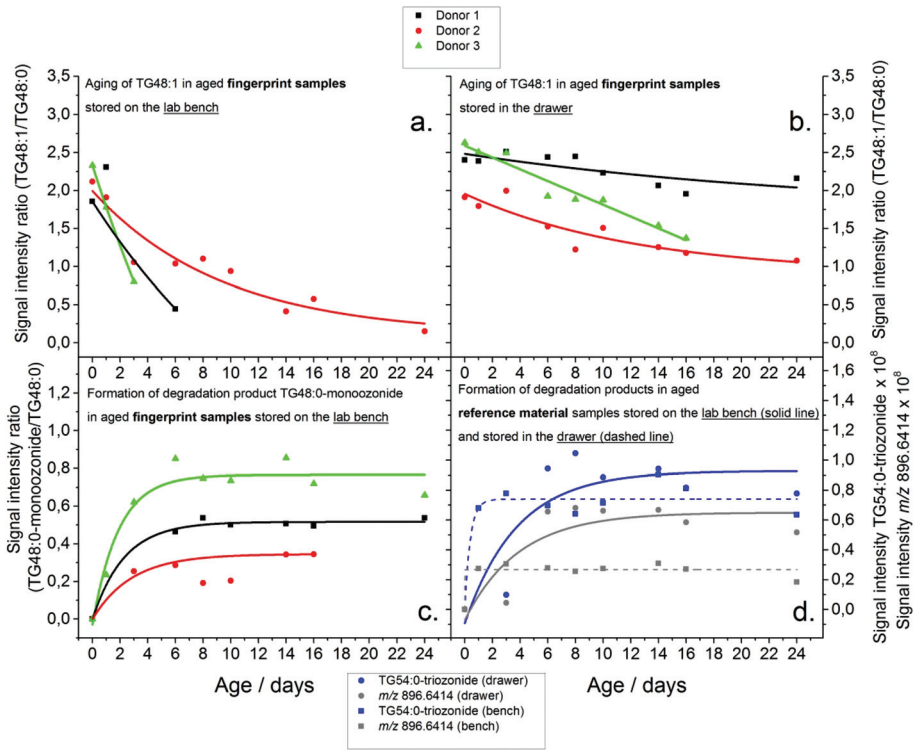

Fig. 7 (a) Aging curves of TG(48:1) in fingerprint samples for three different donors (sample storage: lab bench). (b) Aging curves of TG(48:1) in fingerprint samples for three different donors (sample storage: drawer). (c) Formation curves of TG(48:0)-monoozonide in fingerprint samples for three different donors (sample storage: lab bench). (d) Formation curves of TG(54:0)-triozonide and *m/z* 896.6414 in aged reference material samples (solid line: samples stored on the lab bench, dashed line: samples stored in the drawer). Every point in (a)–(d) represents the measurement of a single sample. Lines are provided to guide the eye.

Although we observed a slight signal intensity decrease of TG(48:1) in light-protected samples, we were not able to detect TG(48:0)-monoozonide as a degradation product in any of these samples. It seems like ozonolysis occurs to some extent in light-protected samples, but the degradation product stays below the limit of detection in analyzed samples.

Fig. 7d shows the formation curves of two different degradation products in aged samples of reference material TG(54:3). As reported previously in this article, TG(54:0)-triozonide was detected as a major degradation product in aged samples of TG(54:3). In Fig. 7d formation curves are presented for samples stored on the lab bench (solid lines) and samples stored in the drawer (dashed lines). In both curves a strong signal intensity increase within 3 days of aging can be observed. It confirms the observation that ozonolysis also occurs in light-protected samples, stored in the drawer. Protecting fingerprint samples from light does not prevent the ozonolysis of unsaturated lipids. Air circulation is reduced in the drawer, which might explain the slower degradation process in fingerprint samples stored in the drawer. Another reason might be the reaction of ozone with volatile compounds (*e.g.* formaldehyde), evaporated out of the wooden drawer material.

Due to the higher concentration of the reference material samples, the ozonide degradation products could be detected in these samples, different from the lower-concentrated fingerprint samples. Fingerprint samples contain many other unsaturated lipids which react with ozone, producing a diversity of lowly concentrated ozonolysis products, below the limit of detection.

Fig. 7d also shows the formation curves for the previously discussed doubly charged ion at *m/z* 896.6414. The formation curves show the same behavior as those of TG(54:0)-triozonide. Signal intensities strongly increased within the first days of aging, both, in the light-protected samples and in the samples exposed to light. The detection of this additional degradation product confirms one of the multiple competing degradation processes, occurring in fingerprint residues. Due to low concentrations, we were not able to identify comparable degradation products in fingerprint samples, but nevertheless competing processes should be considered in the age estimation of fingerprint residues.

Presented findings provide crucial information about fingerprint chemistry in general. They represent substantial progress in method development for age estimation of fingerprints, as we now know major degradation processes of unsaturated lipids.

MALDI-MSI: fingerprint samples

In forensic science, highly sensitive analytical techniques (*e.g.* GC-MS and LC-MS) are used to (chemically) generate evidence

in various investigations. GC-MS is often called the "Gold Standard" in forensic science. Often the sampling methods on a crime scene bear a high risk of contamination and represent a general problem in modern forensic sciences using GC-MS.

Fingerprints are usually visualized by treatment with an adhesion material (*e.g.* carbon powder). Brushes are used to deposit the adhesion material on latent fingerprints for visualization. This method is important to obtain the characteristic pattern of the print for identification purposes. The brush method enables the visualization of fingerprints on large surfaces and often treats several fingerprints with one stroke. The brush, however, may transfer fingerprint ingredients from one fingerprint to another. Assuming the brush picks up ingredients from an aged fingerprint and transfers it to a non-aged fingerprint or *vice versa*, it would be disastrous for a chemical characterization of fingerprints. It would lead to wrong results in the age estimation of fingerprints based on the analysis of the chemical composition. This is the only one example, showing the big problem of some sampling methods in forensics in the context of a subsequent highly sensitive chemical analysis. For this reason it is desirable to develop a method of fingerprint analysis, which investigates the fingerprint pattern, the chemical composition and the age of a fingerprint simultaneously in a single analysis, ideally without contacting the print.

Mass spectrometric imaging generates the fingerprint pattern based on the spatial distribution of natural fingerprint ingredients and thus provides all the above-mentioned information in one measurement. Consequently, it is a powerful method to advance investigation in forensic science, as it combines the visualization of evidence with chemical characterization. In this study MALDI-MSI was performed on non-aged and aged fingerprint samples to show the high potential of this technique for fingerprint chemical analysis. It also provides an additional proof that target compounds, previously identified by LC-MS, originate from the fingerprint pattern.

Lauzon *et al.* reported the identification of numerous di- and triglycerides in fingerprint samples by mass spectrometry imaging.[78] Besides other target compounds, they identified TG(48:1) as a sodium adduct ion in non-aged fingerprint samples.[78] The results of our study are consistent with the reported results. We present here the newly identified TG oxidation products.

Fig. 8a shows the spatial distribution of TG(48:1) as a sodium adduct ion (m/z 827.71009, Δm = 0.20 ppm) in the randomly chosen analyzed area (6250 μm × 6250 μm) of the fingerprint. The m/z image acquired with a 25 μm pixel size has been overlaid with the optical image which was obtained prior to matrix application. As a result of the high spatial resolution, the papillae and the pores are visible in detail in the m/z image of m/z 827.71009. We were able to detect numerous triglycerides using the described method.

In previously reported LC-MS experiments we identified m/z 870.7395 (as ammonium adduct) in aged fingerprint samples as the natural degradation product of TG(48:1) in the course of ozonolysis. For an additional proof of the results from LC-MS

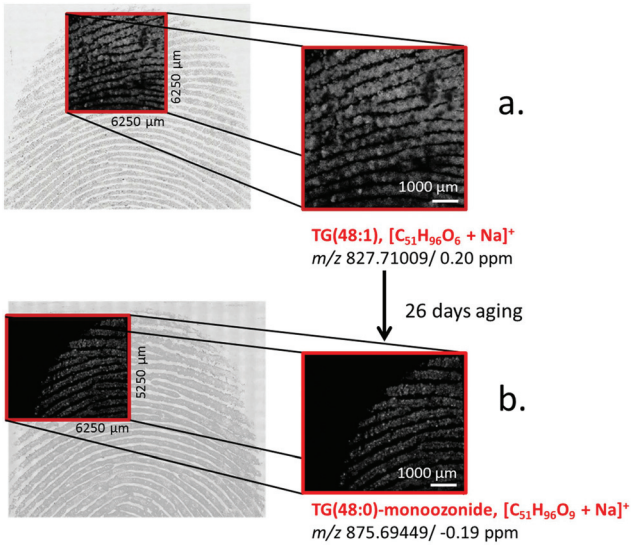

Fig. 8 m/z images overlaid with the optical images of (a) non-aged fingerprint and (b) 26 day aged fingerprint (m/z 827.71009, Δm = 0.20 ppm and m/z 875.69449, Δm = −0.19 ppm).

we analyzed the spatial distribution of TG(48:0)-monoozonide. Fig. 8b shows the m/z image of TG(48:0)-monoozonide as a sodium adduct ion (m/z 875.69449, Δm = −0.19 ppm) in the 26 day old fingerprint sample, overlaid with the corresponding optical image. The spatial distribution of TG(48:0)-monoozonide indicates the degradation of TG(48:1) in the aged sample during lipid ozonolysis. The original lipid TG(48:1) was below the limit of detection in the analyzed sample after 26 days of aging using the reported MSI method.

The triglyceride TG(48:1), with highest intensity in the LC-MS analyses of non-aged fingerprint samples, and its natural degradation product TG(48:0)-monoozonide were assigned in the MALDI-MSI experiments based on the accurate mass detection and spatial distribution of the compounds.

Conclusion

In the present study, we focused on the structure identification of lipid degradation products in aging fingerprint residues. In our previous study we proposed a new approach for the age estimation of fingerprint residues on the basis of the detection of free fatty acids and their corresponding degradation products.[28] The ability to generate characteristic aging markers using signal intensities of unsaturated fatty acids and their natural oxidation products is a tremendous benefit in fingerprint chemical analysis. Due to the importance of this promising approach, we decided to pursue the idea and successfully identified a new class of lipid degradation products in aged fingerprint residues.

In our previous study, we were using GC-MS for our fingerprint analyses.[28] As we were not able to detect non-volatile lipids by using GC-MS, we developed an LC-MS method in this

study for the sensitive detection and reliable identification of triglycerides and their natural oxidation products in fingerprint samples. In our study MALDI-MSI was additionally conducted on non-aged and aged fingerprint samples to show the high potential of this technique in fingerprint chemical analysis. MALDI-MSI provides simultaneous visualization and chemical characterization of fingerprints and is therefore a powerful method for future investigations in forensic science. It also provides an additional proof, that target compounds, previously identified by LC-MS, originate from the fingerprint pattern.

Previous studies mostly focused on artificial triglyceride ozonolysis by an external ozone source. However, few studies analyzed lipid ozonolysis under ambient air conditions. As ozone is one of the most reactive oxygen species in ambient air, it plays a crucial role in the natural aging process of fingerprint residues.

For this reason, we first analyzed the aging behavior of the standard lipid trioctadecenoyl glycerol and found that lipid ozonolysis is the main degradation process under ambient conditions. Degradation was found to begin early, within 2 days of sample exposure to ambient indoor air. As our reference lipid beard three double bonds, we identified three different degradation products. While mono- and diozonides were detected within the first day of aging, the triozonide was found to become the major oxidation product after 2 days. Our findings are consistent with the results reported by Sun *et al.*[50]

Compared to the aging of fingerprint residues, monounsaturated triglycerides have the highest intensity in non-aged fingerprints, even higher than saturated triglycerides. Thus, monounsaturated triglycerides and their degradation pathways were the main focus of this study.

Since fingerprint residues comprise many additional compounds with protective properties (*e.g.* squalene), the degradation rates of fingerprint triglycerides cannot be directly compared with the degradation rates of the reference lipid. Lipid monoozonides were detected immediately after the deposition of fingerprints exposed to atmospheric air.

With the presented aging curves, we show the essential advantage of the relative signal intensity values. As the quantitative compositions of fingerprints differ considerably, the presented relative values provide a more reliable aging marker. It shows the crucial benefit of normalization to the signal intensity of TG(48:0) for this purpose.

The identification of major degradation products was required for the characterization of lipid degradation pathways in fingerprints. The results from aging experiments with the reference material of TG(54:3) and identification of several degradation products proved competing degradation pathways in addition to ozonolysis that have to be considered in the age estimation of fingerprints.

These results are essential for fingerprint chemical analysis, but the number of (environmental) factors influencing the aging of individual compounds poses the most difficult challenge in the development of a method for fingerprint age estimation and limits the use of these results in forensic case work. As discussed in our previous study, it is essential to design aging models which mimic relevant aging conditions to observe the real effects of certain influences. Our study particularly illustrated the tremendous effect of storage conditions during the aging process. Aging curves from the samples stored on the lab bench and those stored in the drawer strongly differed. Whereas the unsaturated triglycerides degraded quickly on the lab bench, signal intensities decreased much slower in the samples stored in the drawer. Several conditions (protection from light, less air circulation) might explain this behavior. For fingerprint age estimation in forensic case work it is indispensable to have knowledge of the effects of relevant influencing factors on individual aging processes.

The presented results provide new and essential information on the chemical compositions of fingerprint residues. In our previous study of aged fingerprint samples, we showed that the newly identified decanal is produced by the oxidation of several unsaturated fatty acids. The herein identified lipid monoozonides, produced in the course of triglyceride aging, represent individual degradation products of particular lipids and bear a crucial advantage for the development of a dating method for fingerprints. The presented values, relative to TG(48:0) as a natural internal standard, can be used as characteristic aging markers, independent of the absolute amount of residues. They represent the degradation of an individual and unique fingerprint ingredient. High-resolution MSI analyses provide the identification of fingerprint ingredients in addition to the generation of characteristic fingerprint patterns for the identification of suspects. Research and method development in fingerprint chemistry combined with MSI will provide a powerful tool for future forensic investigations.

Conflicts of interest

There are no conflicts of interest to declare.

Acknowledgements

The authors gratefully acknowledge financial support from Federal Criminal Police Office Germany (KT 43 and IZ 22) and from Deutsche Forschungsgemeinschaft under DFG grant Sp314/13-1.

References

1 R. M. B. Mackenna, V. R. Wheatley and A. Wormall, The composition of the surface skin fat ('sebum') from the human forearm, *J. Invest. Dermatol.*, 1950, **15**, 33–47.
2 V. R. Wheatley, Studies of Sebum - The estimation of squalene in sebum and sebum-like materials, *Biochem. J.*, 1950, **55**, 637–640.

3 V. R. Wheatley, Studies of Sebum - 5. The Composition of Some Sebum-Like Materials of Human Origin, *Biochem. J.*, 1952, **58**, 167–172.
4 I. S. Hodgson-Jones and V. R. Wheatley, Studies of Sebum - Methods for the Collection and Estimation of Small Amounts of Sebum, *Biochem. J.*, 1952, **52**, 460–464.
5 R. M. B. Mackenna, V. R. Wheatley and A. Wormall, Studies of Sebum - Some Constituents of the Unsaponifiable Matter of Human Sebum, *Biochem. J.*, 1952, **52**, 161–168.
6 A. T. James and V. R. Wheatley, Studies of Sebum - The Determination of the Component Fatty Acids of Human Forearm Sebum by Gas-Liquid Gaschromatography, *Biochem. J.*, 1954, **63**, 269–273.
7 B. Boughton, I. S. Hodgson-Jones, R. M. B. Mackenna, V. R. Wheatley and A. Wormall, Some observations on the nature, origin and possible function of the squalene and other hydrocarbons of human sebum, *J. Invest. Dermatol.*, 1954, **9**, 179–190.
8 B. Boughton, R. M. B. Mackenna, V. R. Wheatley and A. Wormall, Studies of Sebum - 8. Observations on the squalene and cholesterol content and the possible functions of squalene in human sebum, *Biochem. J.*, 1957, **66**, 32–38.
9 B. Boughton and V. R. Wheatley, Studies of Sebum 9. Further studies on the composition of the unsaponifiable matter, *Biochem. J.*, 1957, **73**, 144–149.
10 G. M. Mong, C. E. Petersen and T. R. W. Clauss, *Advanced Fingerprint Analysis Project - Fingerprint Constituents*, Pacific Northwest National Laboratory, Richland, Washington, 1999.
11 R. S. Croxton, M. G. Baron, D. Butler, T. Kent and V. G. Sears, Variation in amino acid and lipid composition of latent fingerprints, *Forensic Sci. Int.*, 2010, **199**, 93–102.
12 R. S. Croxton, M. G. Baron, D. Butler, T. Kent and V. G. Sears, Development of a GC-MS Method for the Simultaneous Analysis of Latent Fingerprint Components, *J. Forensic Sci.*, 2006, **51**, 1329–1333.
13 S. Michalski, R. Shaler and F. L. Dorman, The Evaluation of Fatty Acid Ratios in Latent Fingermarks by Gas Chromatography/Mass Spectrometry (GC/MS) Analysis, *J. Forensic Sci.*, 2013, **58**, 215–220.
14 K. G. Asano, C. K. Bayne, K. M. Horsman and M. V. Buchanan, Chemical composition of fingerprints for gender determination, *J. Forensic Sci.*, 2002, **47**, 805–807.
15 M. V. Buchanan, K. Asano and A. Bohanon, Chemical characterization of fingerprints from adults and children, *Forensic Evid. Anal. Crime Scene Investig. Proc. SPIE 2941*, 1997, **89**, 89–95.
16 A. Girod and C. Weyermann, Lipid composition of fingermark residue and donor classification using GC/MS, *Forensic Sci. Int.*, 2014, **238**, 68–82.
17 M. De Puit, M. Ismail and X. Xu, LCMS Analysis of Fingerprints, the Amino Acid Profile of 20 Donors, *J. Forensic Sci.*, 2014, **59**, 364–370.
18 K. M. Antoine, S. Mortazavi, A. D. Miller and L. M. Miller, Chemical differences are observed in children's versus adults' latent fingerprints as a function of time, *J. Forensic Sci.*, 2010, **55**, 513–518.
19 N. Archer, Y. Charles, J. Elliott and S. Jickells, Changes in the lipid composition of latent fingerprint residue with time after deposition on a surface, *Forensic Sci. Int.*, 2005, **154**, 224–239.
20 G. Popa, R. Potorac and N. Preda, Method for fingerprints age determination, *Rom. J. Leg. Med.*, 2010, **18**, 149–154.
21 C. Weyermann, C. Roux and C. Champod, Initial results on the composition of fingerprints and its evolution as a function of time by GC/MS analysis, *J. Forensic Sci.*, 2011, **56**, 102–108.
22 A. Koenig, A. Girod and C. Weyermann, Identification of wax esters in fingermark residues by GC/MS and their potential use as aging parameters, *J. Forensic Identif.*, 2011, **61**, 1–24.
23 K. Mountfort, H. Bronstein, N. Archer and S. M. Jickells, Identification of oxidation products of squalene in solution and in latent fingerprints by ESI-MS and LC/APCI-MS, *Anal. Chem.*, 2007, **79**, 2650–2657.
24 R. Ramotowski, in *Advances in Fingerprint Technology*, ed. H. C. Lee and R. E. Gaensslen, CRC Press, 2001, pp. 63–104.
25 A. Girod, A. Spyratou, D. Holmes and C. Weyermann, Aging of target lipid parameters in fingermark residue using GC/MS: Effects of influence factors and perspectives for dating purposes, *Sci. Justice*, 2016, **56**, 165–180.
26 A. Girod, R. Ramotowski, S. Lambrechts, P. Misrielal, M. Aalders and C. Weyermann, Fingermark age determinations: legal considerations, review of the literature and practical propositions, *Forensic Sci. Int.*, 2016, **262**, 212–226.
27 A. Girod, R. Ramotowski and C. Weyermann, Composition of fingermark residue: A qualitative and quantitative review, *Forensic Sci. Int.*, 2012, **223**, 10–24.
28 S. Pleik, B. Spengler, T. Schäfer, D. Urbach, S. Luhn and D. Kirsch, Fatty Acid Structure and Degradation Analysis in Fingerprint Residues, *J. Am. Soc. Mass Spectrom.*, 2016, **27**, 1565–1574.
29 E. N. Frankel, Lipid oxidation, *Prog. Lipid Res.*, 1980, **19**, 1–22.
30 N. A. Porter and D. G. Wujek, Autoxidation of Polyunsaturated Fatty Acids, an Expanded Mechanistic Study, *J. Am. Chem. Soc.*, 1984, **106**, 2626–2629.
31 H. Esterbauer, A. Benedetti, J. Lang, R. Fulceri, G. Fauler and M. Comporti, Studies on the mechanism of formation of 4-hydroxynonenal lipid peroxidation during microsomal lipid peroxidation, *Biochim. Biophys. Acta*, 1986, **816**, 154–166.
32 W. Pryor and N. Porter, Suggested mechanisms for the production of 4-hydroxy-2-nonenal from the autoxidation of polyunsaturated fatty acids, *Free Radicals Biol. Med.*, 1990, **8**, 541–543.
33 H. Esterbauer, R. J. Schaur and H. Zollner, Chemistry and Biochemistry of 4-hydroxynonenal, malonaldehyde and related aldehydes, *Free Radicals Biol. Med.*, 1991, **11**, 81–128.

34 K. H. Cheeseman, Mechanisms and effects of lipid peroxidation, *Mol. Aspects Med.*, 1993, **14**, 191–197.
35 E. Niki, Y. Yoshida, Y. Saito and N. Noguchi, Lipid peroxidation: Mechanisms, inhibition, and biological effects, *Biochem. Biophys. Res. Commun.*, 2005, **338**, 668–676.
36 G. Astarita, A. C. Kendall, E. A. Dennis and A. Nicolaou, Targeted lipidomic strategies for oxygenated metabolites of polyunsaturated fatty acids, *Biochim. Biophys. Acta*, 2015, **1851**, 456–468.
37 M. Carini, G. Aldini and R. M. Facino, Mass spectrometry for detection of 4-hydroxy-trans-2-nonenal (HNE) adducts with peptides and proteins, *Mass Spectrom. Rev.*, 2004, **23**, 281–305.
38 C. Wakita, K. Honda, T. Shibata, M. Akagawa and K. Uchida, A method for detection of 4-hydroxy-2-nonenal adducts in proteins, *Free Radicals Biol. Med.*, 2011, **51**, 1–4.
39 R. Domingues, P. Domingues, T. Melo, D. Pérez-Sala, A. Reis and C. M. Spickett, Lipoxidation adducts with peptides and proteins: Deleterious modifications or signaling mechanisms? J, *Proteomics*, 2013, **92**, 110–131.
40 P. Jørgensen, L. Milkovic, N. Zarkovic, G. Waeg and S. I. S. Rattan, Lipid peroxidation-derived 4-hydroxynonenal-modified proteins accumulate in human facial skin fibroblasts during ageing in vitro, *Biogerontology*, 2014, **15**, 105–110.
41 X. Zhu, X. Tang, V. E. Anderson and L. M. Sayre, Mass spectrometric characterization of protein modification by the products of nonenzymatic oxidation of linoleic acid, *Chem. Res. Toxicol.*, 2009, **22**, 1386–1397.
42 C. F. Schönbein, Ueber verschiedene chemische Zustaende des Sauerstoffs, *Ann. Phys. Chem.*, 1847, **71**, 517–530.
43 C. D. Harries, Ueber die Einwirkung des Ozons auf organische Verbindungen, *Justus Liebigs Ann. Chem.*, 1905, **343**, 311–344.
44 R. Criegee, Die Ozonolyse, *Chem. Unserer Zeit*, 1973, **7**, 75–81.
45 R. Criegee, Mechanism of Ozonolysis, *Angew. Chem., Int. Ed. Engl.*, 1975, **14**, 745–752.
46 M. C. Thomas, T. W. Mitchell and S. J. Blanksby, Ozonolysis of Phospholipid Double Bonds during Electrospray Ionization: A New Tool for Structure Determination, *J. Am. Chem. Soc.*, 2006, **128**, 58–59.
47 B. Poad, H. Pham, M. Thomas, J. Nealon, J. Campbell, T. Mitchell and S. Blanksby, Ozone-Induced Dissociation on a Modified Tandem Linear Ion-Trap: Observations of Different Reactivity for Isomeric Lipids, *J. Am. Soc. Mass Spectrom.*, 2010, **21**, 1989–1999.
48 S. H. J. Brown, T. W. Mitchell and S. J. Blanksby, Analysis of unsaturated lipids by ozone-induced dissociation, *Biochim. Biophys. Acta, Mol. Cell Biol. Lipids*, 2011, **1811**, 807–817.
49 K. a. Harrison and R. C. Murphy, Direct mass spectrometric analysis of ozonides: application to unsaturated glycerophosphocholine lipids, *Anal. Chem.*, 1996, **68**, 3224–3230.
50 C. Sun, Y. Y. Zhao and J. M. Curtis, A study of the ozonolysis of model lipids by electrospray ionization mass spectrometry, *Rapid Commun. Mass Spectrom.*, 2012, **26**, 921–930.
51 T. W. Mitchell, H. Pham, M. C. Thomas and S. J. Blanksby, Identification of double bond position in lipids: From GC to OzID, *J. Chromatogr. B: Anal. Technol. Biomed. Life Sci.*, 2009, **877**, 2722–2735.
52 V. B. O'Donnell, Mass spectrometry analysis of oxidized phosphatidylcholine and phosphatidylethanolamine, *Biochim. Biophys. Acta, Mol. Cell Biol. Lipids*, 2011, **1811**, 818–826.
53 A. Ravandi, A. Kuksis, J. J. Myher and L. Marai, Determination of lipid ester ozonides and core aldehydes by high-performance liquid chromatography with on-line mass spectrometry, *J. Biochem. Biophys. Methods*, 1995, **30**, 271–285.
54 G. L. Squadrito, R. M. Uppu, R. Cueto and W. A. Pryor, Production of the criegee ozonide during the ozonation of 1-Palmitoyl-2-oleoyl-sn-glycero-3-phosphocholine liposomes, *Lipids*, 1992, **27**, 955–958.
55 C. Sun, Y.-Y. Zhao and J. M. Curtis, The direct determination of double bond positions in lipid mixtures by liquid chromatography/in-line ozonolysis/mass spectrometry, *Anal. Chim. Acta*, 2013, **762**, 68–75.
56 A. Wisthaler and C. J. Weschler, Reactions of ozone with human skin lipids: Sources of carbonyls, dicarbonyls, and hydroxycarbonyls in indoor air, *Proc. Natl. Acad. Sci. U. S. A.*, 2010, **107**, 6568–6575.
57 D. R. Fooshee, P. K. Aiona, A. Laskin, J. Laskin, S. A. Nizkorodov and P. F. Baldi, Atmospheric Oxidation of Squalene: Molecular Study Using COBRA Modeling and High-Resolution Mass Spectrometry, *Environ. Sci. Technol.*, 2015, **49**, 13304–13313.
58 C. J. Weschler, Ozone in indoor environments: concentration and chemistry, *Indoor Air*, 2000, **10**, 269–288.
59 A. C. Allan and R. Fluhr, Ozone and Reactive Oxygen Species, *Encycl. Life Sci.*, 2001, 1–6.
60 S. R. Ellis, J. R. Hughes, T. W. Mitchell, M. i. H. Panhuis and S. J. Blanksby, Using ambient ozone for assignment of double bond position in unsaturated lipids, *Analyst*, 2012, **137**, 1100–1110.
61 N. Gladovic, L. Zupancic-Kralj and J. Plavec, Determination of primary oxidation products of linoleic acid and triacylglycerols, *J. Chromatogr., A*, 1997, **767**, 63–68.
62 W. C. Byrdwell and W. E. Neff, Dual parallel electrospray ionization and atmospheric pressure chemical ionization mass spectrometry (MS), MS/MS and MS/MS/MS for the analysis of triacylglycerols and triacylglycerol oxidation products, *Rapid Commun. Mass Spectrom.*, 2002, **16**, 300–319.
63 W. C. Byrdwell and W. E. Neff, Autoxidation products of normal and genetically modified canola oil varieties determined using liquid chromatography with mass spectrometric detection, *J. Chromatogr., A*, 2001, **905**, 2006.
64 W. Neff and W. Byrdwell, (Triolein, Trilinolein and Trilinolenin) Autoxidation Products Via High-Performance Liquid Chromatography Coupled With Atmospheric

Pressure Chemical Ionization Mass, *J. Chromatogr., A*, 1998, **818**, 169–186.

65 A. Kuksis, J. P. Suomela, M. Tarvainen and H. Kallio, Lipidomic analysis of glycerolipid and cholesteryl ester autooxidation products, *Mol. Biotechnol.*, 2009, **42**, 224–268.

66 F. Giuffrida, F. Destaillats, L. H. Skibsted and F. Dionisi, Structural analysis of hydroperoxy- and epoxy-triacylglycerols by liquid chromatography mass spectrometry, *Chem. Phys. Lipids*, 2004, **131**, 41–49.

67 Y. Zhou, *et al.* Rapid separation and characterisation of triacylglycerols in ostrich oil by ultra performance liquid chromatography coupled with quadrupole time-of-flight mass spectrometry, *Food Chem.*, 2013, **141**, 2098–2102.

68 K. Ikeda, Y. Oike, T. Shimizu and R. Taguchi, Global analysis of triacylglycerols including oxidized molecular species by reverse-phase high resolution LC/ESI-QTOF MS/MS, *J. Chromatogr. B: Anal. Technol. Biomed. Life Sci.*, 2009, **877**, 2639–2647.

69 J. Ito, S. Mizuochi, K. Nakagawa, S. Kato and T. Miyazawa, Tandem Mass Spectrometry Analysis of Linoleic and Arachidonic Acid Hydroperoxides via Promotion of Alkali Metal Adduct Formation, *Anal. Chem.*, 2015, **87**, 4980–4987.

70 A. Zeb, Chemistry and liquid chromatography methods for the analyses of primary oxidation products of triacylglycerols, *Free Radical Res.*, 2015, **49**, 549–564.

71 D. K. Macmillan and R. C. Murphy, Analysis of Lipid Hydroperoxides and Long-Chain Conjugated Keto Acids by Negative Ion Electrospray Mass Spectrometry, *J. Am. Soc. Mass Spectrom.*, 1995, **6**, 1190–1201.

72 R. Merkel, S. Gruhn, J. Dittmann, C. Vielhauer and A. Bräutigam, On non-invasive 2D and 3D Chromatic White Light image sensors for age determination of latent fingerprints, *Forensic Sci. Int.*, 2012, **222**, 52–70.

73 D. R. Ifa, N. E. Manicke, A. L. Dill and R. G. Cooks, Latent fingerprint chemical imaging by mass spectrometry, *Science*, 2008, **321**, 805.

74 R. Wolstenholme, R. Bradshaw, M. R. Clench and S. Francese, Study of latent fingermarks by matrix-assisted laser desorption/ionisation mass spectrometry imaging of endogenous lipids, *Rapid Commun. Mass Spectrom.*, 2009, **23**, 3031–3039.

75 S. Francese, R. Bradshaw, L. S. Ferguson, R. Wolstenholme, M. R. Clench and S. Bleay, Beyond the ridge pattern: multi-informative analysis of latent fingermarks by MALDI mass spectrometry, *Analyst*, 2013, **138**, 4215–4228.

76 E. Patel, M. R. Clench, A. West, P. S. Marshall, N. Marshall and S. Francese, Alternative Surfactants for Improved Efficiency of In Situ Tryptic Proteolysis of Fingermarks, *J. Am. Soc. Mass Spectrom.*, 2015, **26**, 862–872.

77 C. Elsner and B. Abel, Ultrafast High-Resolution Mass Spectrometric Finger Pore Imaging in Latent Finger Prints, *Sci. Rep.*, 2014, **4**, 6905.

78 N. Lauzon, M. Dufresne, V. Chauhan and P. Chaurand, Development of Laser Desorption Imaging Mass Spectrometry Methods to Investigate the Molecular Composition of Latent Fingermarks, *J. Am. Soc. Mass Spectrom.*, 2015, **26**, 878–886.

79 G. B. Yagnik, A. R. Korte and Y. J. Lee, Multiplex mass spectrometry imaging for latent fingerprints, *J. Mass Spectrom.*, 2013, **48**, 100–104.

80 S. Muramoto and E. Sisco, Strategies for Potential Age Dating of Fingerprints through the Diffusion of Sebum Molecules on a Nonporous Surface Analyzed Using Time-of-Flight Secondary Ion Mass Spectrometry, *Anal. Chem.*, 2015, **87**, 8035–8038.

81 S. Muramoto, T. P. Forbes, A. C. van Asten and G. Gillen, Test Sample for the Spatially Resolved Quantification of Illicit Drugs on Fingerprints Using Imaging Mass Spectrometry, *Anal. Chem.*, 2015, 150507140441002, DOI: 10.1021/acs.analchem.5b01060.

82 K. Kaplan-Sandquist, M. A. LeBeau and M. L. Miller, Chemical analysis of pharmaceuticals and explosives in fingermarks using matrix-assisted laser desorption ionization/time-of-flight mass spectrometry, *Forensic Sci. Int.*, 2014, **235**, 68–77.

83 W. Bouschen, O. Schulz, D. Eikel and B. Spengler, Matrix vapor deposition/recrystallization and dedicated spray preparation for high-resolution scanning microprobe matrix-assisted laser desorption/ionization imaging mass spectrometry (SMALDI-MS) of tissue and single cells, *Rapid Commun. Mass Spectrom.*, 2010, **24**, 355–364.

84 M. Koestler, D. Kirsch, A. Hester, A. Leisner, S. Guenther and B. Spengler, A high-resolution scanning microprobe matrix-assisted laser desorption/ionization ion source for imaging analysis on an ion trap/Fourier transform ion cyclotron resonance mass spectrometer, *Rapid Commun. Mass Spectrom.*, 2008, **22**, 3275–3285.

85 C. Paschke, A. Leisner, A. Hester, K. Maass, S. Guenther, W. Bouschen and B. Spengler, Mirion–a software package for automatic processing of mass spectrometric images, *J. Am. Soc. Mass Spectrom.*, 2013, **24**, 1296–1306.